Journal of Nuclear Medicine, published on September 13, 2018 as doi:10.2967/jnumed.118.217885

Three-hour delayed imaging improves assessment of coronary ^{18}F-sodium fluoride PET.

Jacek Kwiecinski[1,2], Daniel S Berman[1], Sang-Eun Lee[3], Damini Dey[1], Sebastien Cadet[1], Martin L Lassen[1], Guido Germano[1], Maurits A Jansen[2], Marc R Dweck[2], David E Newby[2], Hyuk-Jae Chang[3], Mijin Yun[3*], Piotr J Slomka*[1]

*joint senior authors

1 Cedars-Sinai Medical Center, Los Angeles, CA, USA;

2 BHF Centre for Cardiovascular Science, Clinical Research Imaging Centre, Edinburgh Heart Centre, University of Edinburgh, Edinburgh, United Kingdom

3 Severance Cardiovascular Hospital, Yonsei University College of Medicine, Seoul, South Korea

Corresponding Authors

Piotr J. Slomka, PhD

Artificial Intelligence in Medicine Program

Cedars-Sinai Medical Center

8700 Beverly Blvd, Ste A047N

Los Angeles, CA 90048, USA

Email: piotr.slomka@cshs.org

Phone: 310-423-4348 Fax: 310-423-0173

Mijin Yun, MD, PhD

Department of Nuclear Medicine,

Severance Hospital, Yonsei University College of Medicine,

50-1 Yonsei-ro, Seodaemun-gu, Seoul 03722, Korea

Email: YUNMIJIN@yuhs.ac

Phone: +82-2-2228-2350 Fax: +82-2-312-0578

First Author

Jacek Kwiecinski, MD

Cedars-Sinai Medical Center

8700 Beverly Blvd, S Mark Taper Foundation Imaging Center # A238

Los Angeles, CA 90048

Email: jacek.kwiecinski@cshs.org

Phone: 310-423-7679 Fax: 310-423-8396

Word count: 4988

Financial support:

This research was supported in part by grant R01HL135557 from the National Heart, Lung, and Blood Institute/National Institute of Health (NHLBI/NIH). The content is solely the responsibility of the authors and does not necessarily represent the official views of the National Institutes of Health.

The study was also supported by a grant ("Cardiac Imaging Research Initiative") from the Miriam & Sheldon G. Adelson Medical Research Foundation.

Brief title: Delayed ^{18}F-NaF PET imaging.

ABSTRACT

Coronary ^{18}F-sodium fluoride (^{18}F-NaF) PET imaging identifies ruptured plaques in patients with recent myocardial infarction and localizes to atherosclerotic lesions with active calcification. Most studies to date performed the PET acquisition 1-hour (1h) post-injection. Although qualitative and semi-quantitative analysis is feasible with 1h images, often residual blood pool activity makes it difficult to discriminate plaques with ^{18}F-NaF uptake from noise. We aimed to assess whether delayed 3-hour (3h) post-injection PET scan improves image quality and uptake measurements.

Methods

Twenty patients (67±7years old, 55% male) with stable coronary artery disease underwent coronary CT angiography and PET/CT both 1 h and 3 h after the injection of 266.2±13.3 MBq of ^{18}F-NaF. We compared the visual pattern of coronary uptake, maximal background(blood pool) activity, noise, standard uptake values (SUVmax), corrected SUV (cSUVmax) and target to background (TBR) measurements in lesions defined by CTA on 1h vs 3h post injection ^{18}F-NaF PET.

Results

On 1h PET 26 CTA lesions with ^{18}F-NaF PET uptake were identified in 12 (60%) patients. On 3h PET we detected ^{18}F-NaF PET uptake in 7 lesions which were not identified on the 1h PET. The median cSUVmax and TBR values of these lesions were 0.48 [interquartile range (IQR) 0.44-0.51] and 1.45 [IQR, 1.39-1.52] compared to -0.01 [IQR, -0.03-0.001] and 0.95 [IQR, 0.90-0.98] on 1h PET, both $p<0.001$. Across the entire cohort 3h PET SUVmax values were similar to 1h PET measurements 1.63 [IQR, 1.37-1.98] vs. 1.55 [IQR, 1.43-1.89], $p=0.30$ and the

background activity was lower 0.71 [IQR, 0.65-0.81] vs. 1.24 [IQR, 1.05-1.31], p<0.001. On 3h PET, the TBR values, cSUVmax and the noise were significantly higher (2.30 [IQR, 1.70-2.68] vs 1.28 [IQR, 0.98-1.56], p<0.001; 0.38 [IQR, 0.27-0.70] vs 0.90 [IQR, 0.64-1.17], p<0.001 and 0.10 [IQR, 0.09-0.12] vs. 0.07 [IQR, 0.06-0.09], p=0.02). The median cSUVmax and TBR values increased by 92% (range: 33-225%) and 80% (range: 20-177%).

Conclusions

Blood-pool activity decreases on delayed imaging facilitating the assessment of ^{18}F-NaF uptake in coronary plaques. The median target to background ratios increase by 80% leading to the detection of more plaques with significant uptake compared to the standard 1h protocol. A greater than a 1h delay may improve the detection of ^{18}F-NaF uptake in coronary artery plaques.

Keywords

PET/CT

Coronary artery imaging

Delayed imaging

Coronary artery disease

^{18}F-NaF

Introduction

Coronary ^{18}F-sodium fluoride (^{18}F-NaF) PET imaging depicts biological processes involved in plaque formation and rupture in patients with coronary artery disease (*1*). Increased ^{18}F-NaF uptake has been observed with hybrid PET (positron emission tomography)/coronary CT angiography (CTA) to localize in regions of recent plaque rupture in patients with acute myocardial infarction as well as in coronary plaques with high-risk features on intravascular ultrasound in patients with stable coronary artery disease (CAD) (*2*). As this promising imaging approach is still in its infancy, several technical aspects regarding ^{18}F-NaF coronary PET imaging remain to be addressed (*3,4*).

In the 1970s when ^{18}F-NaF was first used for bone scanning, Blau et al suggested that the optimal scanning time for ^{18}F-NaF is 2-4 hours post injection (*5,6*). Nevertheless, whole-body ^{18}F-NaF PET is nowadays most often performed with imaging commencing 60 minutes after injection (*7-10*). In cardiovascular PET, in most studies to date assessing ^{18}F-NaF uptake in atherosclerotic plaques, acquisition was performed 1-hour (1h) after tracer administration (*1,2,11-13*). Although semi-quantitative analysis is feasible with 1h images, it can be difficult to discriminate plaques with ^{18}F-NaF uptake from noise. Recently, it has been speculated that the optimal time for atherosclerotic plaque imaging with ^{18}F-sodium fluoride might differ from the 1h post injection time-point used for bone imaging (*13*). Up to date only one study looked at the optimal timing for cardiovascular ^{18}F-NaF imaging, but performed the ungated low-count PET acquisition measuring overall uptake in the entire heart rather than in coronary plaques (*14*). In this study, we aimed to quantitatively assess whether delayed 3-hour (3h) post-injection state-of-the-art PET scanning improves image quality and coronary ^{18}F-NaF uptake measurements.

Materials and Methods

Patients

We analyzed scans of 20 patients with stable coronary artery disease who underwent coronary CTA and PET/CT imaging both 1h and 3h after a single injection of ^{18}F-NaF at Severance Cardiovascular Hospital. All study participants had angiographically proven CAD (defined as at least one >50% luminal stenosis). Exclusion criteria included, renal dysfunction (eGFR ≤30 mL/min/1.73 m2), contraindication to iodinated contrast agents, significant ventricular or atrial arrhythmia (which could compromise image quality), class III congestive heart failure and ejection fraction <35%. The study was approved by the investigational review board, and written informed consent was obtained from all enrolled patients.

Imaging acquisition and reconstruction

PET

All patients underwent ^{18}F-NaF PET/CT on a hybrid PET-CT scanner (Discovery 710, GE Healthcare, Milwaukee, WI, USA). Prior to imaging, subjects were administered with a target dose of 250 MBq of ^{18}F-NaF and rested in a quiet environment for 60 minutes. After the acquisition of a non-contrast attenuation correction scan, PET data was acquired in list mode for 30 minutes. The list mode dataset was reconstructed using a standard ordered expectation maximization algorithm with resolution recovery (SharpIR). Corrections were applied for attenuation, dead time, scatter and random coincidences. Utilizing 10 cardiac gates, the data were reconstructed on a 256x256 matrix (20x20cm field of view) using 24 subsets and applying 4 iterations along with 5mm Gaussian smoothing. For standard uptake value (SUV) assessment, all analyzed values were decay-corrected to the injection time.

CT angiography

After the 1h PET acquisition, contrast-enhanced coronary CTA was performed with prospective ECG-triggering if the heart rate was <60 beats/min and regular or with ECG gated helical acquisition if the heart rate >60 beats/min or irregular. All patients received beta blockers and sublingual nitrates. For contrast-enhanced imaging iodinated contrast (65-130ml) was power injected at 5-6 ml/sec, followed by a saline flush. Transverse images were reconstructed using filtered back projection with 0.65-mm slice thickness, 0.4 mm increment, and a medium-soft convolution kernel.

Delayed PET

A second low-dose CT for attenuation correction and PET was performed 3h after tracer administration using the same protocol for imaging and the same reconstruction of PET datasets as used in the 1h study.

PET Motion correction

Cardiac motion correction was performed on the 1h and 3h ^{18}F-NaF PET/CT data. This technique compensates for coronary artery motion by aligning all gates to the end-diastolic position and has demonstrated its ability to reduce image noise and improve target to background ratio (TBR) (*15*). First, anatomic coronary artery data was extracted from diastolic coronary CTA by applying a vessel tracking algorithm based on Bayesian maximal paths using dedicated software (Autoplaque version 2.0, Cedars-Sinai Medical Center). Second, a diffeomorphic mass-preserving image registration algorithm was used to align the 10 gates of PET data to the end-diastolic gate (gate 7 or 8 dependent on the timing of the CTA acquisition). After motion correction, the 10 gates were summed to build a motion-free image containing counts from the entire PET acquisition.

Image analysis

Coronary CTA

Evaluation of coronary artery plaques was conducted in accordance with the Society of Cardiovascular Computed Tomography guidelines (*16*). The extent of disease was characterized by lesion maximal stenosis (Autoplaque version 2.0, Cedars-Sinai Medical Center), plaque composition (non-calcified/partially calcified/totally calcified), the segment involvement score (SIS) and coronary calcium scoring (*17,18*).

PET

Coronary ^{18}F-NaF image analysis was performed on axial images using FusionQuant Software (Cedars Sinai Medical Center, Los Angeles). PET and CTA reconstructions were reoriented, fused and systematically co-registered in all 3 planes. Key points of reference were the sternum, vertebrae, blood pool in the ventricles and the great vessels. For each scan, plaque activity was measured by delimiting 3-dimensional volumes of interest on lesions. All segments with coronary plaque (at least a grade 2 stenosis [>25%]) and a lumen diameter ≥2 mm, as defined by CTA were interrogated. The maximum standard uptake value (SUVmax) was recorded from all these segments by delimiting a spherical volume of interest (radius=5mm). Background blood pool activity (SUVmean) was measured by delimiting a cylindrical volume of interest (radius=10mm, thickness = 5mm) in the right atrium on the level of the right coronary artery orifice (*19*). TBRs were calculated by dividing SUVmax by averaged background blood pool activity. Corrected maximum standard uptake values (cSUVmax) were calculated by subtracting the blood-pool activity from SUVmax. Image noise was defined as the coefficient of variance of the blood pool activity. Coronary plaques were considered clearly positive for ^{18}F-NaF uptake if they presented with focal tracer uptake arising from the coronary plaque which followed the course of the vessel in three dimensions over more than one slice and had a TBR>1.25 (*2*). In

addition to reporting decay corrected uptake values we also evaluated the raw counts. The PET acquisitions were analyzed independently with at least a 21-day interval between the reading of the 1h and the 3h after injection scan.

Statistical Analysis

Continuous data are expressed as mean (standard deviation) or median [interquartile range (IQR)] as appropriate. Parametric data were compared using student's T-test and paired student's T-test, non-parametric data were compared using Wilcoxon rank sum and Wilcoxon signed-rank test where appropriate. Categorical variables are presented as absolute numbers (percentage) and were compared using a Chi-squared test or Fisher's exact test where appropriate. A two-sided p value <0.05 was considered statistically significant. Statistical analyses were performed using SPSS (version 24, IBM, USA) software.

Results

Twenty patients (67±7 years old, 55% male) were recruited into the study. Patient baseline characteristics are shown in Table 1. On CTA, the median segment involvement and coronary calcium scores were 6 [IQR, 3-8] and 413 [IQR, 50-770] respectively. Exact PET tracer injected doses were 266.2±13.3 MBq of ^{18}F-NaF.

1h post injection imaging

On 1h PET (acquisition 66.5 [IQR, 64.5-71.8] min post injection), coronary uptake exceeding the TBR=1.25 threshold was observed in 12 (60%) patients. Twenty-six CTA segments were considered positive for ^{18}F-NaF uptake. Eleven (41%) were in the left anterior descending, 6 (23%) in the left circumflex, 4 (16%) in the left main and 5 (20%) in the right coronary artery. The association between patients' baseline characteristics, risk-profiles and CTA findings are presented in supplementary Tables S1 and S2.

3h post injection imaging

On delayed PET imaging (acquisition 180.5 [IQR, 177.3-193.0] min post injection), by visual inspection background ^{18}F-NaF activity was markedly reduced, and coronary lesions were more conspicuous. We identified all segments which were detected on 1h post injection imaging (Figure 1). In addition, 7 new segments (median stenosis 48.6% [IQR, 35.7-60.2]) which were previously negative for ^{18}F-NaF uptake demonstrated focal uptake with TBR>1.25 (Figure 2). These lesions were found in 2 patients who had uptake elsewhere in the coronary vasculature and in 3 patients classified as negative for ^{18}F-NaF coronary uptake on 1h post injection imaging. While the SUVmax of these 7 new positive lesions was similar on 3h vs 1h PET (1.51 [IQR, 1.42-1.60] vs. 1.48 [IQR, 1.40-1.55], p=0.68), the cSUVmax and TBR values were higher on

delayed imaging (0.48 [IQR, 0.44-0.51] vs. -0.01 [IQR, -0.03-0.001] and 1.45 [IQR, 1.39-1.52] vs. 0.95 [IQR, 0.90-0.98], both $p<0.001$).

Across the entire cohort on 3h PET compared to 1h PET, the SUVmax of the detected lesions remained similar (1.63 [IQR, 1.37-1.98] vs. 1.55 [IQR, 1.43-1.89], $p=0.30$). However, the background activity decreased to 0.71 [IQR, 0.65-0.81] vs. 1.24 [IQR, 1.05-1.31], $p<0.001$ with a median decrease of 42% (range 18-48%). Consequently, the TBR values were higher (2.30 [IQR, 1.70-2.68] vs 1.28 [IQR, 0.98-1.56], $p<0.001$), with a median TBR increase of 80% (range: 20-177%, Figures: 3 and 4). A similar change was observed in the cSUVmax 0.38 [IQR, 0.27-0.70] vs 0.90 [IQR, 0.64-1.17], $p<0.001$; median cSUVmax increased by 92% (range: 33-225%, Figures 3 and 4). In accordance with the Poisson's distribution, we observed a 49.0±3.8% decrease in counts on delayed imaging compared to 1h PET. As expected due to fewer counts on 3h PET, noise increased 0.10 [IQR, 0.09-0.12] vs. 0.07 [IQR, 0.06-0.09], $p=0.02$.

Discussion

This is the first study which utilized a 30min acquisition cardiac-gated coronary PET protocol and compared the image quality and quantitative measures of ^{18}F-NaF coronary uptake on 1h vs 3h post injection PET images. We hereby show that prolonging the time from tracer injection to PET acquisition can facilitate image analysis and provide lower background activity, higher TBR and cSUV values compared to the currently utilized protocol. We demonstrate that by delaying image acquisition to 3h new lesions, categorized as false-negative on the 1h PET, were now readily identified.

By utilizing currently used imaging protocols with PET acquisition (1h post injection), the reader is often challenged to distinguish true coronary uptake from overspill from the surrounding structures. A large proportion of ^{18}F-NaF positive plaques present with uptake which is at or only slightly higher than the background activity. Visualization of these lesion is usually possible because of below blood-pool activity in the adjacent myocardium. However, analysis can often be difficult particularly in the proximal and mid-LAD which lies close to blood pool in the pulmonary artery (Figure 1) and in the proximal circumflex that lies adjacent to the left atrial appendage. Techniques to improve the detection of such lesions are therefore required. To some extent blurring of the tracer uptake which occurs due to cardiorespiratory and patient motion can be mitigated with end-diastolic imaging, improving the conspicuousness of lesions (*1*). Recently developed cardiac motion correction techniques further improve image quality by co-registration of all cardiac gates to the reference one and allowing all PET data rather than that from a single diastolic gate to be utilized (*15*). In this study, we show that delaying ^{18}F-NaF coronary image acquisition further facilitates assessment of coronary uptake, predominantly as a result of a decrease in the background blood pool activity.

Improved visual identification of the lesions on the delayed ^{18}F-NaF PET acquisition is accompanied by significant improvements in TBR and corrected SUVmax measurements. While the coronary SUVmax remained unchanged on 3h PET imaging, the TBR values improved significantly. We observed an increase in the noise on delayed imaging (as expected due to a lower count statistic), however given the favorable decrease in the background (blood pool) activity, the noise level on 3h PET does not impede image analysis.

The benefit of delayed PET acquisition for the detection of disease is widely appreciated in oncological applications with ^{18}F-fluorodeoxyglucose (FDG)(*20-24*). There is good agreement that because background activity decreases on delayed imaging, the image quality improves. The lower background activity is a critical feature and advantage of delayed imaging, because it increases target to background ratios (*25-26*). It has been shown that a longer time window from injection to acquisition translates to higher signal to noise and therefore facilitates visual analysis providing higher diagnostic accuracy (*20*). For coronary PET imaging, it was suggested that the optimal timing for acquisition with FDG is 2.5-3h after tracer administration (*27,28*).

In case of ^{18}F-NaF PET bone imaging, since it has faster blood clearance and higher bone uptake compared to 99mTc-methylene diphosphonate, the SNM practice guideline recommends emission scanning for the axial skeleton as soon as 30-45 minutes after injection in patients with normal renal function (*10*) to decrease the overall time of the study. However, a longer waiting time of 90-120 minutes was recommended to acquire high-quality images of the extremities. Compared to uptake in the bony skeleton, ^{18}F-NaF uptake due to active microcalcification formation in coronary plaque is very small in amount. Therefore, it is not surprising that a higher TBR in coronary plaques is observed with a longer waiting time from injection to acquisition. Longer delays for cardiovascular ^{18}F-NaF PET imaging were evaluated by only one study to date

(14). Blomberg et al. concluded that delayed ^{18}F-NaF PET imaging does not improve quantification of vascular calcification. However, the authors measured only overall heart ^{18}F-NaF activity (including blood pool) by placing regions of interest around the cardiac silhouette on ungated PET/CT images (excluding ^{18}F-NaF activity originating from bones and cardiac valves), and averaged the SUV values derived from all slices. As a result, identifying additional foci of uptake on delayed imaging was not feasible. Moreover, that study was performed without cardiac gating and motion correction. Further, with 2.5-minute scan time and a 2.2 MBq dose of ^{18}F-NaF per kilogram of body weight the authors had approximately 16 times less counts compared to our coronary scans (~3.4MBq dose per kg and 30-min long acquisition).

The utilization of coronary CT angiography in our study enabled measuring ^{18}F-NaF uptake in individual coronary plaques. It also provided an opportunity to evaluate potential predictors of uptake by means of regression modelling (supplemental Tables S1 and S2). While our study is slightly underpowered such analysis revealed that TBR is positively associated with partially calcified plaque and inversely with lipid lowering drugs (statins). These findings are in line with previously published data showing that active calcification, macrophage infiltration and partially calcified plaques are associated with ^{18}F-NaF uptake (2,29). On the contrary in our study completely calcified plaques did not attract the PET tracer which is in accordance with prior studies and supports the view that ^{18}F-NaF is a marker active calcification including the stage before the development of advanced atherosclerotic lesions rather than established disease (30,31). Interestingly, as shown by the explanatory uni- and multivariate analysis the associations with clinical and imaging data are stronger when 3h PET measures rather 1h post injection PET values are utilized (Tables S1 and S2).

Our findings have important clinical implications. Given the challenges that ^{18}F-NaF imaging faces, which include, but are not limited to small target lesion size, cardiac, respiratory and gross patient motion which collectively compromise image quality, a delayed acquisition protocol is an important step in mitigating the modest TBR reported in studies utilizing the 1h post injection protocol. By decreasing the background (blood pool) signal, not only do the TBR values improve, but also lesions which were difficult to detect 1h post injection can be easily identified. Additionally, by utilizing the 3 hours' post injection approach coronary uptake can be more readily assessed by less experienced readers. In our view, such a protocol can facilitate dissemination of this imaging techniques beyond academic institutions.

Limitations

We acknowledge that our study was based on a modest number of patients with stable CAD. Importantly, despite this limitation our findings are supported by statistically significant data. The normal limits applied to define an increase in TBR values in our population were based on those derived from 1h data; thus, it is likely that reference values for relevant uptake on 3h ^{18}F-NaF coronary PET will need to be derived for optimal use of delayed imaging (1,2). The utilization of TBR as a measure of tracer uptake remains to some degree controversial (32); however, we also evaluated corrected SUVmax measurements which have been suggested to be more robust for coronary imaging. The low TBR values in our study can be attributed to partial volume effects as adjacent myocardium presents on average with 60% of the blood-pool uptake (33). We acknowledge that a 3h post injection PET protocol may lead to reorganizing the workflow within the nuclear medicine imaging facility and will prolong the time patients spend in the imaging facility. Nevertheless, the benefits of delayed PET acquisition for the assessment

of ^{18}F-NaF coronary uptake undoubtedly outweigh the aforementioned workflow inconveniences.

Conclusions

Blood-pool activity decreases on delayed imaging facilitating the assessment of ^{18}F-NaF uptake in coronary plaques. It increases the corrected SUVmax and target to background ratios on average by 92% (range: 33-225%) and 80% (range: 20-177%), leading to the detection of more plaques with clear increases in uptake compared to the standard 1h protocol. A greater than a 1h delay may improve the detection of ^{18}F-NaF uptake in coronary artery plaques.

Financial Disclosure

This research was supported in part by grant R01HL135557 from the National Heart, Lung, and Blood Institute/National Institute of Health (NHLBI/NIH). The content is solely the responsibility of the authors and does not necessarily represent the official views of the National Institutes of Health.

The study was also supported by a grant ("Cardiac Imaging Research Initiative") from the Miriam & Sheldon G. Adelson Medical Research Foundation.

References

1. Dweck MR, Chow MW, Joshi NV, et al. Coronary arterial 18F-sodium fluoride uptake: a novel marker of plaque biology. J Am Coll Cardiol 2012; 59(17): 1539-48.

2. Joshi NV, Vesey AT, Williams MC, et al. 18F-fluoride positron emission tomography for identification of ruptured and high-risk coronary atherosclerotic plaques: a prospective clinical trial. Lancet 2014; 383: 705-13.

3. Adamson PD, Vesey AT, Joshi NV, Newby DE., Dweck MR. Salt in the wound: (18)F-fluoride positron emission tomography for identification of vulnerable coronary plaques. Cardiovasc Diagn Ther 2015;5:150–155,

4. Thomas GS, Haraszti RA. A new frontier in atherosclerotic coronary imaging. Lancet 2014;383:674-5.

5. Blau M, Ganatra R, Bender MA. 18 F-fluoride for bone imaging. Semin Nucl Med. 1972;2:31–37.

6. Blau M, Nagler W, Bender MA. Fluorine-18: a new isotope for bone scanning. J Nucl Med. 1962;3:332–334.

7. Grant FD, Fahey FH, Packard AB, Davis RT, Alavi A, Treves ST. Skeletal PET with 18F-fluoride: applying new technology to an old tracer. J Nucl Med. 2008;49:68–78.

8. Hawkins RA, Choi Y, Huang SC, et al. Evaluation of the skeletal kinetics of fluorine-18-fluoride ion with PET. J Nucl Med. 1992;33:633–642.

9. Czernin J, Satyamurthy N, Schiepers C. Molecular mechanisms of bone 18F-NaF deposition. J Nucl Med. 2010;51:1826–1829.

10. Segall G, Delbeke D, Stabin MG, et al. SNM practice guideline for sodium 18Ffluoride PET/CT bone scans 1.0. J Nucl Med. 2010;51:1813–1820.

11. Derlin T, Toth Z, Papp L, et al. Correlation of inflammation assessed by 18F-FDG PET, active mineral deposition assessed by 18F-Fluoride PET, and vascular calcification in atherosclerotic plaque: a dual-tracer PET/CT study. J Nucl Med. 2011;52:1020–1027.

12. Derlin T, Richter U, Bannas P, et al. Feasibility of 18F-sodium fluoride PET/CT for imaging of atherosclerotic plaque. J Nucl Med. 2010;51:862–865.

13. Derlin T, Wisotzki C, Richter U, et al. In vivo imaging of mineral deposition in carotid plaque using 18F-sodium fluoride PET/CT: correlation with atherogenic risk factors. J Nucl Med. 2011;52:362–368.

14. Blomberg BA, Thomassen A, Takx RA et al. Delayed sodium 18F-fluoride PET/CT imaging does not improve quantification of vascular calcification metabolism: results from the CAMONA study. J Nucl Cardiol 2014;21:293-304.

15. Rubeaux M, Joshi N, Dweck MR, et al. Motion correction of 18F-sodium fluoride PET for imaging coronary atherosclerotic plaques.; J Nucl Med 2016;57:54–9.

16. Leipsic J, Abbara S, Achenbach S, et al. SCCT guidelines for the interpretation and reporting of coronary CT angiography: a report of the Society of Cardiovascular Computed Tomography Guidelines Committee. J Cardiovasc Comput Tomogr 2014;8:342–58.

17. Min JK, Shaw LJ, Devereux RB, et al. Prognostic value of multidetector coronary computed tomographic angiography for prediction of all-cause mortality. J Am Coll Cardiol 2007;50:1161–70.

18. Agatston AS, Janowitz WR, Hildner FJ, Zusmer NR, Viamonte M Jr, Detrano R. Quantification of coronary artery calcium using ultrafast computed tomography. J Am Coll Cardiol 1990;15:827–32.

19. Pawade TA, Cartlidge TR, Jenkins WS et al. Optimization and reproducibility of aortic valve . Circ Cardiovasc Imaging 2016; 9: e005131

20. Kubota K, Itoh M, Ozaki K, et al. Advantage of delayed whole-body FDG-PET imaging for tumour detection. Eur J Nucl Med. 2001; 28:696–703.

21. Caoduro C, Porot C, Vuitton DA, Bressonhadni S, Grenouillet F. The role of delayed 18F-FDG PET imaging in the follow-up of patients with alveolar echinococcosis. J. Nucl. Med.2013;54:1–6.

22. Kubota K, Yokoyama J, Yamaguchi K, et al. FDG-PET delayed imaging for the detection of head and neck cancer recurrence after radio-chemotherapy comparison with MRI/CT. Eur J Nucl Med Mol Imaging 2004:31:590–95

23. Nishiyama Y, Yamamoto Y, Monden T, Sasakawa Y, Tsutsui K, Wakabayashi H, Ohkawa M. Evaluation of delayed additional FDG PET imaging in patients with pancreatic tumour. Nucl Med Commun. 2005;26:895–901.

24. LinW-Y,Tsai S-C, Hung G-U. Value of delayed 18F-FDG-PET imaging in the detection of hepatocellular carcinoma. Nuclear Med Comm 2005;26:315–321.

25. Cheng G, Torigian DA, Zhuang H, Alavi A. When should we recommend use of dual time-point and delayed time-point imaging techniques in FDG PET? Eur J Nucl Med Mol Imaging. 2013;40:779-87.

26. Houshmand S, Salavati A, Segtnan EA, Grupe P, Høilund-Carlsen PF, Alavi A. Dual-time-point Imaging and Delayed-time-point Fluorodeoxyglucose-PET/Computed Tomography Imaging in Various Clinical Settings. PET Clin. 2016;11:65-84.

27. Rudd JH, Warburton EA, Fryer TD, et al. Imaging atherosclerotic plaque inflammation with [18F]-fluorodeoxyglucose positron emission tomography. Circulation. 2002;105:2708–2711.

28. Bucerius J, Mani V, Moncrieff C, et al. Optimizing 18F-FDG-PET/CT imaging of vessel wall inflammation: the impact of 18F-FDG circulation time, injected dose, uptake parameters, and fasting blood glucose levels. Eur J Nucl Med Mol Imaging. 2014;41:369–383

29. Kitagawa T, Yamamoto H, Toshimitsu S et al. 18F-sodium fluoride positron emission tomography for molecular imaging of coronary atherosclerosis based on computed tomography analysis. Atherosclerosis 2017;263:385-392.

30. McKenney-Drake ML, Territo PR, Salavati A et al. 18F-NaF PET Imaging of Early Coronary Artery Calcification. JACC Img 2016;9:627-628

31. Oliveira-Santos M, Castelo-Branco M, Silva R et al. Atherosclerotic plaque metabolism in high cardiovascular risk subjects - a subclinical atherosclerosis imaging study with 18F-NaF PET-CT. Atherosclerosis 2017;260:41-46

32. Chen W, Dilsizian V. PET assessment of vascular inflammation and atherosclerotic plaques: SUV or TBR? J Nucl Med. 2015;56:503–4.

33. Abgral R, Trivieri M, Dweck M et al. Assessment of cardiac amyloidosis by using 18f-sodium fluoride PET/MR imaging. Med Nuc 2017;41(3):148-149

Tables:

Table 1. Patients' baseline clinical characteristics.

	Study cohort (n=20)	SD, IQR, %
Baseline Characteristics		
Age, years	67	±7
Males, n (%)	11	(55%)
Diabetes, n (%)	4	(20%)
Hyperlipidemia, n (%)	5	(25%)
Hypertension, n (%)	12	(60%)
Tobacco use, n (%)	6	(30%)
Family history of CAD, n (%)	3	(15%)
Serum Biomarkers		
Total Cholesterol	162	[135-189]
HDL	43	[38-46]
LDL	93	[71-107]
Triglyceride	121	[86-140]
Creatine	0.8	[0.7-0.9]
Medications		
Aspirin, n (%)	13	(65%)
Statin, n (%)	6	(30%)
ACEI/ARB, n (%)	6	(30%)
Beta Blocker, n (%)	7	(35%)
Leading clinical indication for CTA		
Chest pain, n (%)	15	(75%)
Dyspnea, n (%)	3	(15%)
Risk assessment (asymptomatic patient), n (%)	2	(10%)

Coronary Computed Tomography Angiography		
Segment involvement score	6	[3-8]
Multivessel disease, n (%)	6	(30%)
Coronary calcium score	312	[50-770]

CAD: coronary artery disease; CTA: coronary computed tomography angiography; HDL – high density lipoprotein; LDL – low density lipoprotein; ACEI – angiotensin converting enzyme inhibitor; ARB – angiotensin receptor blocker; SD – standard deviation; IQR - Interquartile range.

Table 2. Comparison of ^{18}F-NaF motion corrected measurements on 1h and 3h post injection PET imaging.

	1-hour post injection PET	3-hour post injection PET	P Value
SUVmax	1.55 [1.43-1.89]	1.63 [1.37-1.98]	0.30
TBR	1.28 [0.98-1.56]	2.30 [1.70-2.68]	<0.001
Corrected SUVmax	0.38 [0.27-0.70]	0.90 [0.64-1.17]	<0.001
Background (blood pool)	1.24 [1.05-1.31]	0.71 [0.65-0.81]	<0.001
Noise	0.07 [0.06-0.09]	0.10 [0.09-0.12]	0.02
Segments with TBR>1.25, n (%)	26 (8%)	33 (10%)	0.01
Patients with TBR>1.25, n (%)	12 (60%)	15 (75%)	0.004

^{18}F-NaF: ^{18}F-sodium fluoride; PET: positron emission tomography; SUVmax: maximum standard uptake values; TBR: maximum target to background ratios.

FIGURE 1. Assessment of ^{18}F-NaF coronary uptake on 1h and 3h delayed PET.

Four patients with significant (TBR>1.25) on 1h post injection (left column) coronary uptake in the left anterior descending artery. Uptake can be difficult to differentiate in this region from blood pool in the adjacent pulmonary artery. On 3h PET (right column) the TBR increased significantly, and blood pool activity reduced improving image quality.

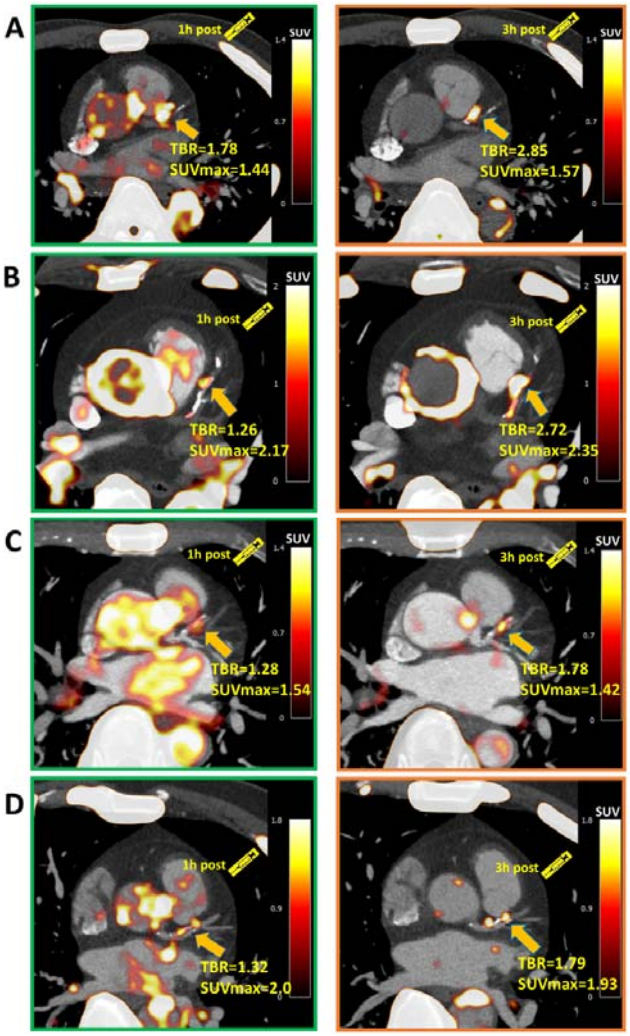

^{18}F-NaF: ^{18}F-sodium fluoride; PET: positron emission tomography; TBR: target to background ratios; SUV: standard uptake value

FIGURE 2. Examples of coronary plaques with significant uptake on 3h PET and low tracer activity of 1h post injection imaging.

Short axis images of proximal left anterior descending, proximal circumflex (A) and distal right coronary artery (B) plaques which had a TBR<1.0 on 1h PET (left column) and showed uptake exceeding the 1.25 TBR threshold at 3h

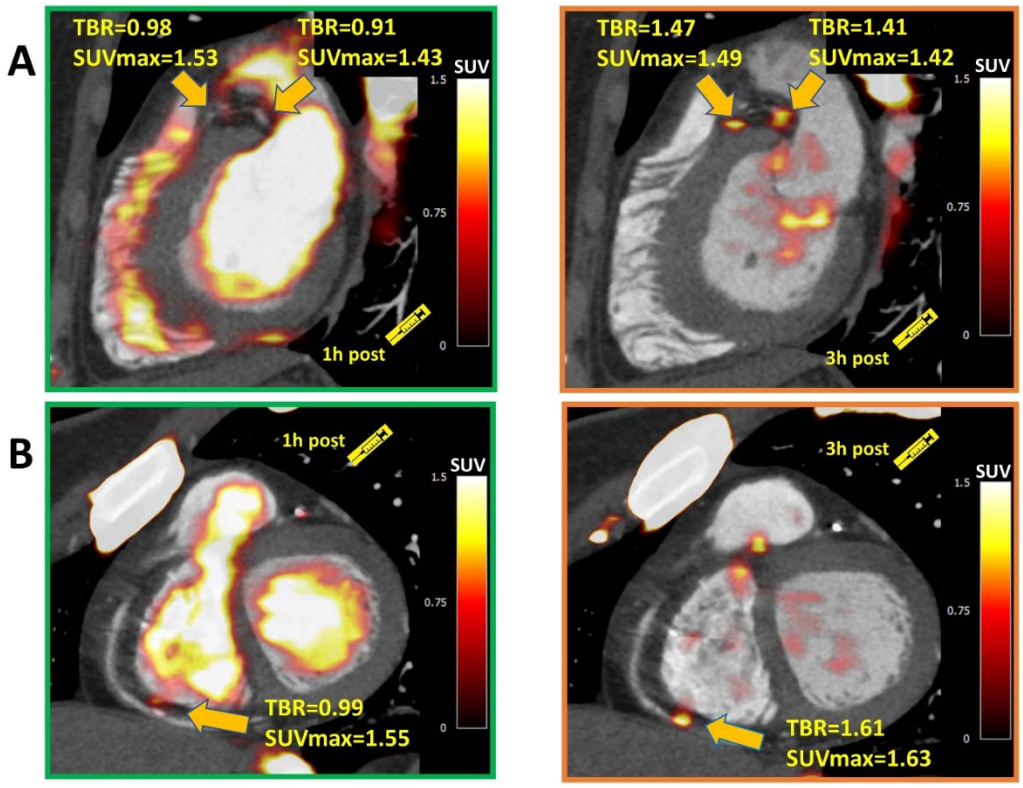

TBR: target to background ratios; PET: positron emission tomography

FIGURE 3. ^{18}F-NaF coronary uptake measures on 1h and 3h delayed PET.

Maximum standard uptake values (SUVmax) values were comparable on both scans (A). The corrected SUVmax and target to background (TBR) values were higher on 3h post injection PET (B,C). The background (right atrium blood pool SUVmean) was lower on 3h imaging (D).

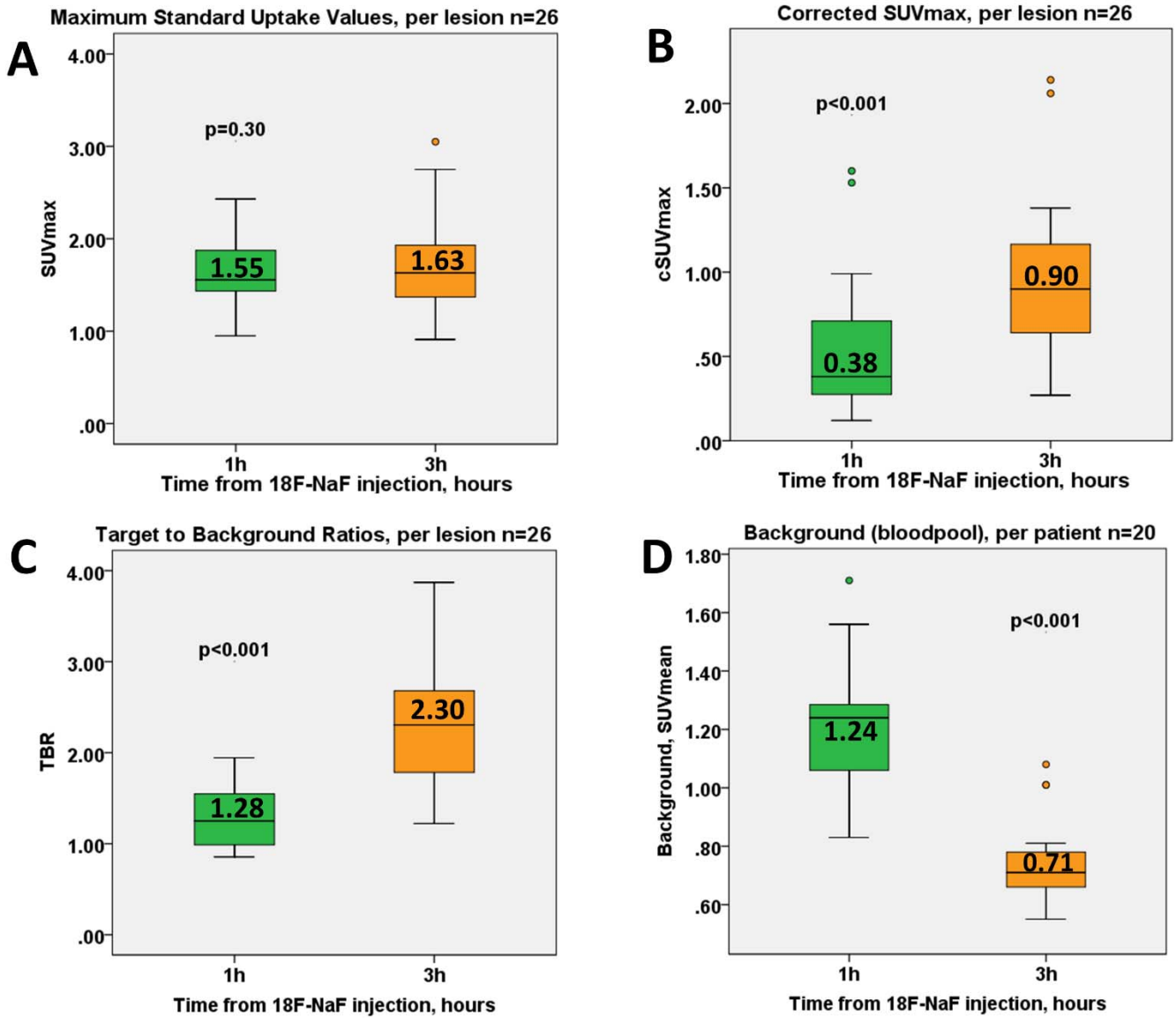

PET: positron emission tomography; ^{18}F-NaF: ^{18}F-sodium fluoride

Figure 4 Line-plots of ^{18}F-NaF coronary uptake measurements on 1h and 3h delayed PET. Maximum standard uptake values (SUVmax) values were comparable on both scans (A). The corrected SUVmax and target to background (TBR) values were higher on 3h post injection PET (B,C). The background (right atrium blood pool SUVmean) was lower on 3h imaging (D).

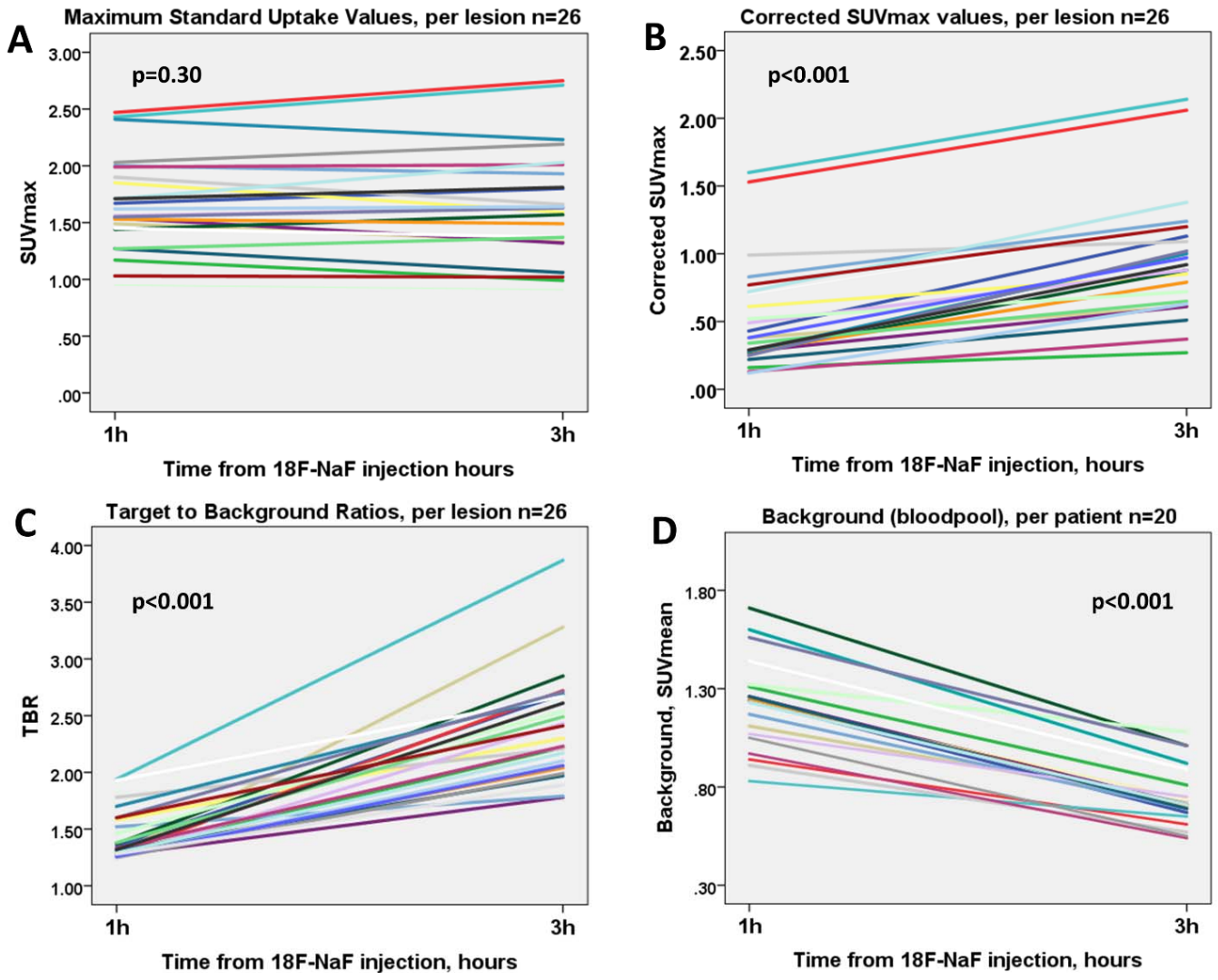

PET: positron emission tomography; ^{18}F-NaF: ^{18}F-sodium fluoride

Table S1. Univariate and multivariate linear regression analysis to examine association of variables with maximum per patient 1h post injection target to background uptake measurements. Both multivariate models with: LDL levels, segment involvement scores, presence of multivessel disease, coronary calcium scores and quantitative stenosis. Model 1 additionally includes lipid lowering treatment; Model 2 includes partially calcified plaques.

Variables	Univariate		Multivariable – Model 1 (included: lipid lowering treatment)		Multivariable – Model 2 (included: plaque composition - mixed)	
	Relative change in TBR (95% CI)	P value	Relative change in TBR (95% CI)	P value	Relative change in TBR (95% CI)	P value
LDL	0.001 (-0.001-0.001)	0.97	0.001 (-0.006-0.005)	0.74	0.001 (-0.005-0.006)	0.80
Lipid lowering treatment	-0.30 (-0.60—0.004)	0.047	-0.331 (-0.68-0.023)	0.064		
Segment involvement score	0.04 (-0.05 – 0.67)	0.22	0.01 (-0.06-0.02)	0.53	0.02 (-0.03-0.06)	0.49
Multivessel disease	0.05 (-0.21-0.31)	0.30	0.09 (-0.43-0.27)	0.65	0.33 (-0.01-0.76)	0.11
Coronary calcium score	0.01 (0.001-0.02)	0.39	0.01 (-0.01-0.02)	0.43	0.01 (-0.01-0.02)	0.55
Stenosis	0.001 (-0.007 – 0.10)	0.75	0.002 (-0.007-0.011)	0.66	0.003 (-0.005-0.12)	0.44
Partially calcified plaque	0.30 (0.03-0.57)	0.030			0.56 (0.1-1.0)	0.020

CI: confidence interval, LDL: low density lipoprotein, TBR: maximum target to background ratios.

Table S2. Univariate and multivariate linear regression analysis to examine association of variables with maximum per patient 3h post injection target to background uptake measurements. Both multivariate models with: LDL levels, segment involvement scores, presence of multivessel disease, coronary calcium scores and quantitative stenosis. Model 1 additionally includes lipid lowering treatment; Model 2 includes partially calcified plaques.

Variables	Univariate		Multivariable – Model 1 (included: lipid lowering treatment)		Multivariable – Model 2 (included: plaque composition - mixed)	
	Relative change in TBR (95% CI)	P value	Relative change in TBR (95% CI)	P value	Relative change in TBR (95% CI)	P value
LDL	0.004 (-0.007-0.015)	0.43	0.002 (-0.01-0.01)	0.66	0.01(-0.001-0.015)	0.15
Lipid lowering treatment	-0.32 (-0.61--0.03)	0.041	-0.36 (-1.04-0.012)	0.079		
Segment involvement score	0.012 (-0.08-0.10)	0.78	0.04 (-0.05-0.13)	0.33	0.03 (-0.04-0.09)	0.40
Multivessel disease	0.09 (-0.61-0.79)	0.21	0.11 (-0.56-0.78)	0.32	0.67 (0.2-1.33)	0.02
Coronary calcium score	0.001 (-0.01-0.011)	0.37	0.001(-0.002-0.003)	0.77	0.001 (-0.001-0.002)	0.79
Stenosis	0.12 (-0.05-0.029)	0.15	0.1 (-0.01-0.03)	0.19	0.02 (0.001-0.03)	0.11
Partially calcified plaque	0.79 (0.27-1.30)	0.005			1.3 (0.7-1.9)	<0.001

CI: confidence interval, LDL: low density lipoprotein, TBR: maximum target to background ratios.